General and Comparative Endocrinology 233 (2016) 88–99

Contents lists available at ScienceDirect

General and Comparative Endocrinology

journal homepage: www.elsevier.com/locate/ygcen

Insulin-like signaling (IIS) responses to temperature, genetic background, and growth variation in garter snakes with divergent life histories

Dawn M. Reding *, Elizabeth A. Addis [1], Maria G. Palacios [2], Tonia S. Schwartz [3], Anne M. Bronikowski

Department of Ecology, Evolution, and Organismal Biology, Iowa State University, Ames, IA 50011, USA

ARTICLE INFO

Article history:
Received 6 September 2015
Revised 26 April 2016
Accepted 11 May 2016
Available online 12 May 2016

Keywords:
Insulin-like growth factor
Thamnophis elegans
Life history
Ecotype
Differential expression
Common garden experiment

ABSTRACT

The insulin/insulin-like signaling pathway (IIS) has been shown to mediate life history trade-offs in mammalian model organisms, but the function of this pathway in wild and non-mammalian organisms is understudied. Populations of western terrestrial garter snakes (*Thamnophis elegans*) around Eagle Lake, California, have evolved variation in growth and maturation rates, mortality senescence rates, and annual reproductive output that partition into two ecotypes: "fast-living" and "slow-living". Thus, genes associated with the IIS network are good candidates for investigating the mechanisms underlying ecological divergence in this system. We reared neonates from each ecotype for 1.5 years under two thermal treatments. We then used qPCR to compare mRNA expression levels in three tissue types (brain, liver, skeletal muscle) for four genes (*igf1*, *igf2*, *igf1r*, *igf2r*), and we used radioimmunoassay to measure plasma IGF-1 and IGF-2 protein levels. Our results show that, in contrast to most mammalian model systems, *igf2* mRNA and protein levels exceed those of *igf1* and suggest an important role for *igf2* in postnatal growth in reptiles. Thermal rearing treatment and recent growth had greater impacts on IGF levels than genetic background (i.e., ecotype), and the two ecotypes responded similarly. This suggests that observed ecotypic differences in field measures of IGFs may more strongly reflect plastic responses in different environments than evolutionary divergence. Future analyses of additional components of the IIS pathway and sequence divergence between the ecotypes will further illuminate how environmental and genetic factors influence the endocrine system and its role in mediating life history trade-offs.

1. Introduction

Species show remarkable variation in life history characteristics such as growth, maturation, reproduction, and lifespan, and biologists are increasingly interested in the importance of ecological divergence (i.e., divergent natural selection on traits between environments that vary in resource availability, predators, disease, physical conditions, etc.) as a mechanism promoting such diversity (Orr and Smith, 1998; Schluter, 2001; Rundle and Nosil, 2005). Despite the variety of environmental selective pressures acting on a wide range of life history phenotypes, many potential combinations of life history traits are not actually observed in nature (Charnov, 1993; Ricklefs, 2000; Ricklefs and Wikelski, 2002). Rather, traits tend to co-vary systematically, a phenomenon that has led to the concept of a "slow-fast continuum" of life history variation: organisms that grow slowly, exhibit lower reproductive rate, and live longer occupy the slow end of the continuum, whereas organisms with the opposite traits fall out at the fast end of the continuum (Stearns, 1983; Promislow and Harvey, 1990). Life history traits are subject to intrinsic trade-offs (Stearns, 1989), but the mechanistic underpinnings of such trade-offs are far from clear (Flatt and Heyland, 2011). The consistent correlation of entire suites of traits, exemplified by the slow-fast continuum, suggests that there may be a shared pleiotropic control mechanism that constrains variation in life history strategies.

The endocrine system plays an integral role in energy allocation and mediates diverse physiological responses to the environment, leading many researchers to posit pleiotropic hormonal pathways as candidate mechanisms underlying life history trade-offs and

* Corresponding author at: Department of Biology, Luther College, Decorah, IA 52101, USA.
E-mail address: redida01@luther.edu (D.M. Reding).
[1] Present address: Department of Biology, Gonzaga University, Spokane, WA 99258, USA.
[2] Present address: Centro Nacional Patagonico, CONICET, Boulevard Brown 2915, Puerto Madryn, Chubut 9120, Argentina.
[3] Present address: Auburn University, Department of Biological Sciences, Auburn, AL 36849 USA.

http://dx.doi.org/10.1016/j.ygcen.2016.05.018
0016-6480/

correlated traits (Ketterson and Nolan, 1992; Ricklefs and Wikelski, 2002; Dantzer and Swanson, 2012). Extensive study in laboratory model organisms and domesticated animals has accrued a compelling case for the role of the IIS pathway in mediating such life history trade-offs (Swanson and Dantzer, 2014; reviewed in Tatar et al., 2003; Bartke, 2005; Dantzer and Swanson, 2012). Two specific ligands of the IIS system – insulin-like growth factors 1 and 2 – can trigger cellular survival, growth, proliferation, migration, and differentiation. By regulating such responses across diverse tissue types, the IGFs play a central role in overall growth, development, reproduction, and lifespan (Stewart and Rotwein, 1996). In vertebrates, the extracellular components of this complex and evolutionarily conserved system consists primarily of two peptide hormones (IGF-1, IGF-2) that are paralogous with and structurally similar to insulin, their cell surface receptors (IGF-1R and IGF-2R, though they also interact with IR), and a family of at least six high-affinity ligand-binding proteins (IGFBP-1 to 6) and their proteases (Denley et al., 2005; Annunziata et al., 2011).

The actions of both IGF-1 and IGF-2 are primarily mediated via binding to IGF-1R, a member of the tyrosine kinase superfamily of transmembrane receptors (Ewton et al., 1987). In contrast, IGF-2R, a mannose 6-phosphate receptor, is generally thought to lack signal transduction capacity (but see El-Shewy et al., 2007) and instead acts as a sink for IGF-2, decreasing its bioavailability to bind IGF-1R (Denley et al., 2005). The IGFs also exhibit some cross-reactivity with the insulin receptor (IR) and hybrid IGF-1R/IR receptors, though typically with lower binding affinity (Nakae et al., 2001). The IGFBPs help to modulate IGF action and can both enhance (increasing the half-life of circulating IGFs and aiding in delivery of IGFs to receptors) and inhibit (sequestering IGFs) their activity (Clemmons, 2003). Circulating IGFs are primarily derived from the liver, but virtually all tissue types are known to produce these hormones and likely exert autocrine and paracrine effects (D'Ercole et al., 1984; Yakar et al., 1999). Thus, both endocrine and local sources of IGF-1 – and potentially IGF-2 – may be important in regulating growth and other postnatal traits in vertebrates.

Although laboratory and domestic animal studies have provided direction and a solid framework for understanding the structure, function, and regulation of IGFs, studies in wild organisms are necessary to illuminate the role that the IGF signaling pathway plays in natural systems. In addition, broader taxonomic representation across vertebrates is needed to illuminate the evolutionary patterns of this system. Only a few studies, however, have investigated the link between IGF-1 and life history characters in natural populations of non-mammalian vertebrates (e.g., Sparkman et al., 2009; reviewed by Dantzer and Swanson, 2012), with even fewer focused on IGF-2 (e.g., Peterson et al., 2004; Schrader and Travis, 2012).

In this study we used a laboratory reciprocal transplant study to test for the effects of temperature, growth, and genetic background on components of the IIS extracellular system. We conducted our study in neonates of garter snakes from a natural system where populations have diverged along a slow-to-fast life history continuum. The western terrestrial garter snakes (*Thamnophis elegans*) of the Eagle Lake basin (Lassen County, CA, USA) have two distinct habitat types and have evolved two contrasting life-history strategies. The fast-living ecotype found along the rocky lakeshore (L-fast) exhibits faster growth, earlier maturation, larger adult body size, and higher annual reproduction, but shorter median lifespan, when compared to the slow-living ecotype found in the nearby montane meadows (M-slow; Bronikowski and Arnold, 1999; Schwartz and Bronikowski, 2011, 2013). This life history divergence is likely driven by differing thermal regimes (Bronikowski, 2000), resource availability (Miller et al., 2011), and predation rates (Sparkman et al., 2013), with the lakeshore environment experiencing higher mean temperatures, year-to-year stability and abundance of prey, and increased susceptibility to predation.

In an observational study of free-ranging animals, Sparkman et al. (2009) found that circulating IGF-1 protein levels were higher in the L-fast ecotype. Although the findings generally corroborated predictions based on a basic understanding of IGF-1 function in domestic and model organisms, patterns of IGF-1 levels were not clearly dichotomous between the ecotypes but rather depended upon reproductive status, season, and food availability. Given that this study was observational, it was not designed to test whether the differences in plasma IGF-1 levels between the ecotypes were due to adaptive genetic differences or reflected plastic responses in varying environmental conditions (e.g., Sparkman et al., 2010). Furthermore, the importance of other molecules in the IGF system, such as IGF-2 and the receptors, has yet to be explored.

The goals of the present study were three fold. First, we compare mRNA expression levels of *igf1*, *igf2*, *igf1r*, and *igf2r* across several important tissue types and with circulating IGF-1 and IGF-2 protein levels in lab-reared juvenile snakes to gain a better understanding of the IGF system in reptiles. We predicted that liver should have the highest expression of *igf1* and *igf2* if, similar to lab models, it is the main endocrine source of these ligands. We also predicted that *igf1* would be more highly expressed overall than *igf2*, if, as in mammalian studies, *igf1* is the main mitogen responsible for postnatal growth. Second, to tease apart the importance of genetic and environmental effects on the IGF system, we test whether rearing neonates from both ecotypes under two different thermal treatments alters mRNA and protein levels. We predicted that the genes thought to promote growth (*igf1*, *igf2*, and *igf1r*) would be more highly expressed in L-fast than M-slow snakes, whereas *igf2r*, which potentially inhibits growth by degrading IGF-2, may be down-regulated in the L-fast ecotype. We also anticipated that circulating IGF-1, and potentially IGF-2, protein levels would be higher in the L-fast animals. Since IGF levels generally decline with food restriction and lower environmental temperatures in ectotherms (reviewed in Beckman, 2011; Reindl and Sheridan, 2012), we predicted that animals in the cooler rearing treatment group should exhibit lower IGF-1 and IGF-2 protein levels and lower *igf1*, *igf1r*, and *igf2* mRNA levels than those in the warm treatment group. Third, to investigate the link between IGF signaling and postnatal growth, we test for an association between recent growth and IGF signaling. We predicted a positive correlation between growth-promoting elements of the IGF system (*igf1*, *igf1r*, *igf2*, IGF-1, IGF-2) and growth in juvenile snakes.

2. Methods

2.1. Study animals and treatment groups

In June 2010, 44 gravid females were collected from three replicate populations of each of the L-fast and M-slow ecotypes of *T. elegans* (22 L-fast and 22 M-slow). For the study reported here, 13 L-fast and 16 M-slow litters provided study subjects. All females were brought to the laboratory colony at Iowa State University, where they gave birth to N = 257 live offspring from 12 August – 19 September 2010. Within 24 h of birth, offspring were sexed, weighed (g), measured for body length (mm from snout-to-vent, SVL), and moved to individual plastic boxes. Males and females from each litter were split randomly between two daily temperature treatment groups for a fully factorial experimental design of ecotype × rearing treatment × sex. A subset of these offspring from each ecotype × rearing treatment × sex block were randomly selected for focal animals for the present study ($n = 49$) whereas the rest of the juveniles continued in their treatment groups to

monitor long-term IGF and growth results for future studies. In the wild, mean daily temperatures differ between L-fast and higher elevation M-slow populations (Bronikowski and Arnold, 1999). However, the relevant thermal difference between L-fast and M-slow populations is the daily duration of optimally warm retreat sites (Peterson et al., 1993; Huey et al., 1989), which is of longer duration in L-fast populations (up to 16 h of 28 °C sites available) versus M-slow populations (8 h of 28 °C sites). Thus in our laboratory study, we sought to mimic this key difference in thermal regimes – i.e., the duration of access to warmth. Subjects in the warm (mimicking the L-fast environment) rearing treatment ($n = 12$ from L-fast; $n = 12$ from M-slow) were maintained at an ambient temperature of 20 °C and received 16 h/day of supplementary heating (via under-tank heating tape placed on one end of the box). Animals in the cool (mimicking the M-slow environment) treatment ($n = 14$ from L-fast; $n = 11$ from M-slow) were maintained at the same ambient temperature (20 °C) but received only 8 h of supplemental heat per day. During the periods of heat exposure, each tank provided a thermal gradient that ranged from 22 to 32 °C, which enabled the animals to behaviorally regulate their body temperature. During the periods lacking supplemental heat, all tanks (and therefore animals) were at 20 °C. All offspring were kept on a 12:12 light:dark schedule and offered pinky mice, with amount eaten (grams) recorded at every feeding beginning at birth. Animals were maintained in these environments, except for a period of hibernation at 4 °C from January-May 2011.

The subject snakes were measured for body length on 1 November 2011 and again on 12 January 2012 to quantify growth over the short duration prior to measuring components of IIS. These subjects were a sample of a large laboratory study of growth, including an analysis of growth efficiency and metabolism (Gangloff et al., 2015) and a complete colony analysis of food consumption, growth, and body size over the first 4 years of life (E.A. Addis and A.M. Bronikowski, unpublished data). On 19–20 January 2012, 5–6 days post-feeding (and at approximately 1.5 years of age), we euthanized the study subjects via decapitation, exsanguinated them, and performed gross dissections to isolate brain, liver, and de-skinned tail skeletal muscle. These tissues were immediately snap-frozen in liquid nitrogen. The blood samples were kept on ice in heparinized tubes until centrifuged to separate the plasma, which was then snap-frozen in liquid nitrogen. All samples were stored at −80 °C. Treatment of all experimental animals was in accordance with Iowa State University animal care protocol #3-2-5125-J.

2.2. Quantitative PCR

2.2.1. RNA isolation

We used the Qiagen RNAeasy Mini Tissue Kit (Qiagen Cat No. 74104) to isolate RNA according to the manufacturer's instructions, with modifications noted below. The tissue amount used ranged from 16–33 mg for liver, 6–40 mg for brain (used entire organ), and 30–58 mg for muscle. The muscle segments were coarsely ground with a mortar and pestle in liquid nitrogen prior to homogenization. Samples were immediately placed in 50 mL conical tubes containing 1 mL Buffer RLT and 10 μL Beta-mercaptoethanol and thoroughly homogenized. For the muscle, we performed an additional proteinase K treatment for fibrous tissue that involved adding 2 mL RNase-free water and 50 μL of 20 mg/mL proteinase K to the homogenate, incubating for 20 min in a 60 °C water bath, centrifuging at 5000*g* for 5 min, and combining the supernatant with ½ volume of 100% EtOH to capture RNA on the spin column membrane. For brain and liver, we used 60% EtOH for capturing RNA on the spin column membrane due to their high fat content. The protocol included a DNase digestion on the membrane to remove residual genomic DNA. Elution was performed with the kit-supplied RNase free water. The concentration and purity of RNA was determined by spectrophotometry using a NanoDrop (Thermo Scientific). In addition, 2 μL of each sample were run on a 1.2% agarose gel for visualization of 18S and 28S ribosomal RNA bands to verify the integrity of the RNA. Aliquots of RNA were diluted to ~150 ng/μL and stored at -80 °C until assayed.

2.2.2. cDNA synthesis

Individual RNA aliquots were thawed on ice and concentrations quantified again using a NanoDrop. We used the Superscript III First-Strand Synthesis kit (Invitrogen, Cat. # 18080-051) to make cDNA with oligo$(dT)_{20}$ primers. For each sample we used 0.8 μg of total RNA, with the exception of four brain samples with low concentration. We included no template controls (NTC) to detect the potential presence of nucleic acid contamination in the reverse transcription reagents, as well as no reverse transcriptase (no RT) controls to detect the potential presence of genomic DNA contamination in the purified RNA samples. The RNase H step was included at the end of cDNA synthesis to degrade the RNA complement and improve PCR efficiency. We made a "pool" to be used as a positive control by combining 3 μL from each sample. The cDNA samples were stored at −20 °C until use.

2.2.3. qPCR assay design

Primers for *igf1*, *igf2*, *igf1r*, and *igf2r* (Table 1) were designed from sequences obtained from a *T. elegans* transcriptome study (Schwartz et al., 2010; Schwartz and Bronikowski, 2014). Each primer set was designed to target the 3′ end of the mRNA since the 5′ end may be under-represented in long transcripts. Primer sets were also designed to produce an amplicon that spanned an exon-exon junction to inhibit amplification of genomic contamination. We conducted trial assays with melt curve analysis followed by running the product out on an agarose gel to confirm the presence of a single amplicon of the correct size. In addition, the amplicons were purified, sequenced, and confirmed using BLASTn against the GenBank nr database. Amplicon sequences are included as a Supplementary .fasta file.

2.2.4. Standards for absolute quantification

There are two basic quantification methods, *absolute* quantification and *relative* quantification, and each has its advantages and drawbacks (Pfaffl, 2004). In this study, we used an absolute quantification approach that involved calculating the number of gene copies in unknown "test" samples from comparison with a standard curve prepared from a dilution series of linearized plasmids of known concentration. For each gene, we cloned PCR amplicons using the TOPO TA Cloning Kit with pCR 2.1-TOPO vector and One Shot TOP10 Chemically Competent *Escherichia coli* (Invitrogen, Cat. # K4500-40). Purification of the plasmid DNA containing the PCR insert was carried out with the Qiaprep Spin Miniprep kit (Qiagen, Cat. # 27106). We linearized the plasmid using HindIII restriction enzyme to avoid amplification efficiency problems that arise from using supercoiled plasmids (Hou et al., 2010), and quantified the amount of dsDNA using Quant-iT PicoGreen dsDNA Assay Kit (Invitrogen, Cat. # P7589). We used a website calculator (Staroscik, 2004) to estimate copy number from the equation:

$$\text{number of copies} = (\text{amount} * 6.022 \times 10^{23})/(\text{length} * 1 \times 10^{9} * 650)$$

where amount of DNA (ng) was derived from the PicoGreen assay and length (bp) was determined by adding the PCR product length to the size of the plasmid.

For standard curves, we constructed a 7-point 10× serial dilution series in the range of 10^7 to 10 copies per 5 μL or a 9-point

Table 1
Description of the qPCR primers used in assays of four genes.

Gene	Amplicon length (bp)	Primer name	Primer sequence (5′-3′)	Estimated Tm (°C)	Location
igf1	119	IGF1_151.Ex3.qF	GGCCAAGAAACACTTTGTGG	60.43	Exon3
		IGF1_247.Ex4.qR	AGTAGAAGAGGAACGCCTACTGC	60.53	Exon4
igf2	156	IGF2_Ex5.qR	TGTTTCTACCCACAGGCCTAC	59.11	Exon5
		Te_IGF2_AF	TATTGCTGCTTGTGCTCACC	60.02	Exon 4
igf1r	132	IGF1R_Ex13-14.qF	AGTCTGCTGGTTTAGGTTGGAC	59.68	Exon 13–14
		IGF1-R_DR	AACTTGCTGGAGCCAAACTG	60.43	Exon13
igf2r	138	IGF2-R_Ex38.qF	CAATAGTGCCATCTCATTTGG	58.11	Exon38
		IGF2-R_C3R	GGGAAGACACAAAGCTCACC	59.11	Exon39

5× serial dilution series in the range of 10^7 to 25.6 copies. Use of these standard curves allowed us to control for differences in amplification efficiency of the assays and to calculate the "absolute" number of mRNA transcripts to compare across the genes.

2.2.5. Reactions

For each cDNA sample, we made a 1:8 dilution to assay *igf1* and *igf1r*, and a 1:12 dilution to assay *igf2* and *igf2r*. We assayed gene expression for the four genes (Table 2) using quantitative PCR with the GoTaq qPCR Master Mix system containing BRYT Green (Promega, Cat. # A6002) on an Eppendorf Mastercycler Realplex 2 real-time thermal cycler. Reaction volumes were 20 μL and contained 30 nM of forward and reverse primer, 1× master mix, DEPC treated water, and 5 μL diluted cDNA. The thermal cycle program consisted of a 2 min hot start at 95 °C, followed by 40 cycles of 95 °C for 15 s, 58 °C for 30 s, 68 °C for 20 s. A melting curve analysis from 68 to 95 °C was performed after the reaction was completed to confirm the specificity of the assay. All samples, standards, and negative controls were assayed in duplicate. We re-ran samples for which the standard deviation of the quantification cycle (Cq) values between the duplicates was greater than 0.2 cycles. The pooled sample was included on every plate in order to assess inter-plate variation in Cq values.

2.2.6. Determination of copy number

When 100% efficient, PCR exponential amplification (E_{AMP}) will equal 2, reflecting amplicon doubling each cycle. The reliability of the absolute quantification method is dependent upon identical amplification efficiencies of the test samples and absolute standards (Kavanagh et al., 2011), or in mathematically accounting for differences (Gallup, 2011). A common approach is to estimate and compare efficiencies derived from the slope of dilution curves. We calculated E_{AMP} for each absolute plasmid standard curve (E_{AMPa}) by plugging the slope (m), obtained from plotting Cq against $\log_{10}$ starting copy number, into the following equation:

$$E_{AMP_a} = 10^{(-1/m)}$$

However, our target genes were generally expressed at low levels in the snake cDNA, preventing serial dilution across a broad enough range to adequately determine E_{AMP}. Thus, we used the program LinRegPCR (Ramakers et al., 2003; Ruijter et al., 2009) as an alternative approach to calculate exponential amplification for the test samples (E_{AMPs}), as well as for the absolute plasmid standards (to compare with E_{AMPa} derived from serial dilution), based on individual amplification curves. Briefly, raw fluorescence data from samples and standards for each gene were imported from the Eppendorf system, baseline subtraction was performed individually on each sample, and a common Window-of-Linearity (WoL) and fluorescence threshold was set for each gene. PCR efficiencies per sample were calculated based on the slope of the curve within the WoL and Cq values were obtained for each sample by determining the cycle where the amplification curve crossed the fluorescence threshold. We initially calculated mean efficiency values for the standards and each tissue type separately, but efficiencies did not differ among tissues and thus were combined to provide a single estimate of E_{AMPs} for each gene to compare to the respective E_{AMPa}.

To convert Cq values to estimates of starting copy number (X_{0s}) for the samples, we first corrected for differences in PCR efficiency between the samples and absolute standards using the equation described in Gallup (2011):

$$X_{0_s} = E_{AMP_s}^{\left[b_a * log_{E_{AMPs}}(E_{AMP_a}) - Cq_s\right]}$$

where X_{0s} denotes the starting copy number for a given sample, E_{AMPs} denotes mean amplification efficiency for the samples as determined by LinRegPCR, b_a denotes the Y-intercept and E_{AMPa} the amplification efficiency derived from the absolute plasmid dilution curve, and Cq_s denotes the quantification cycle for a given sample. We adjusted for the cDNA dilution factor and the amount of cDNA included in each qPCR reaction. To enable comparison across samples, we normalized the concentrations to the amount of total RNA (ng) put into each reaction.

Table 2
Details of qPCR absolute standard curves and test samples for four genes.

Gene	Sample dilution	Sample Cq range	Avg SD intraplate Cq	Avg SD interplate Cq	Mean E_{AMPs}[a]	Abs std Cq range	Abs std copy range	Equations	R^2	Mean E_{AMPa}[a]	Mean E_{AMPa}[b]
igf1	1:8	22.2–32.7	0.07	0.05	1.891	12.5–32.7	10^7–25.6	Y = −3.5286x + 37.292	0.9988	1.922	1.9204
igf1r	1:8	22.7–30.3	0.04	0.04	1.841	13.2–33.4	10^7–10	Y = −3.6169x + 38.903	0.9868	1.871	1.8901
igf2	1:12	20.0–28.6	0.06	0.06	1.879	11.1–28.9	10^7–100	Y = −3.5180x + 35.925	0.9973	1.913	1.9242
igf2r	1:12	23.4–27.4	0.04	0.04	1.873	12.8–30.7	10^7–100	Y = −3.5573x + 37.727	0.9969	1.890	1.9103

[a] Based on LinRegPCR.
[b] Based on slope of dilution series.

2.3. Radioimmunoassays (RIA)

2.3.1. IGF-1 RIA

We assayed plasma IGF-1 concentrations by radioimmunoassay using GroPep protocol #3002 (GroPep Ltd., Adelaide, Australia), designed for human IGF-1. This assay had been previously validated for *T. elegans* (see Sparkman et al., 2009). Briefly, samples were extracted using an ethanol-acid solution to strip IGFBPs from IGF-1. Concentrations of plasma IGF-1 were determined by competitive binding with ^{125}I labeled IGF-1 (PerkinElmer #NEZ033). Samples were assayed in duplicate in a single assay; intra-assay variation was 7.5%.

2.3.2. IGF-2 RIA

As for IGF-1, we assayed plasma IGF-2 levels using GroPep's protocol #3002, but with several modifications. First, we used human IGF-2 standards, ^{125}I labeled IGF-2 (PerkinElmer #NEX429), and anti-human IGF-2 primary antibody. Second, we doubled the amount of primary antibody, used five times more secondary antibody, a 12% polyethylene glycol solution, and polypropylene rather than glass tubes because ^{125}I IGF-2 sticks to glass (PerkinElmer technical data sheet for product #NEX429). We extracted all samples using the same acid-ethanol solution.

We validated this assay for *T. elegans* by serial dilution and comparing the *T. elegans* and human curves. First, we made a standard curve of human IGF-2 from 1.25 to 20 ng/mL. We then created a 50 μL pool of *T. elegans* plasma and serially diluted it to create a standard curve of solutions with the following dilution factors: undiluted, 1:2, 1:8, 1:64, and 1:1024. Human and *T. elegans* samples were run in duplicate; the percent binding (B/B_0) of human and *T. elegans* ^{125}I IGF-2 are shown in Fig. 1. The serial dilution curves of human and *T. elegans* IGF-2 binding are parallel. For the IGF-2 RIA, all samples were measured in duplicate in a single assay. Intra-assay variation was 9.5%.

2.4. Statistical analyses

All statistical analyses were conducted using SAS 9.3 software (SAS Institute, Cary, NC). Protein variables were $\log_{10}$-transformed, whereas mRNA variables were $\log_2$-transformed to improve fit of residuals to a normal distribution. We removed extreme outliers that were outside the range of Q1 − 3*IQR and Q3 + 3*IQR, where Q1 denotes the first quartile, Q3 the third quartile, and IQR the interquartile range (Q3–Q1). Levels of mRNA in two brain samples were consistently low (classified as extreme outliers) for *igf1r*, *igf2*, and *igf2r*, and data from these two brain samples were removed for all four genes. In addition, data from one muscle sample that was classified as a high outlier for *igf1r*, and two muscle samples classified as low outliers for *igf2* were also removed from further analysis. For the protein levels, only IGF-1 contained extreme outliers, and we omitted data from one low and two high samples.

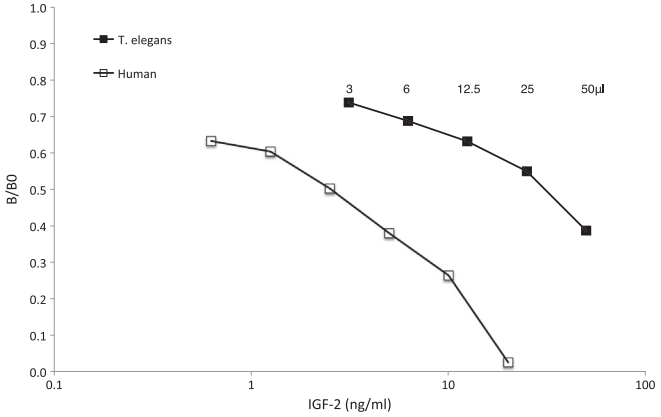

Fig. 1. Validation of a human radioimmunoassay (RIA) for IGF-2 in *Thamnophis elegans*. This figure shows the parallelism of human standards of known concentration and a serial dilution (volumes of pooled plasma above curve, with 50 μL representing the initial undiluted pool) for *T. elegans*. Percent of ^{125}I bound to the antibody (B/B_0) is dependent upon the concentration of human IGF-2.

Preliminary analyses indicated that tissue type was the primary driver of the observed variation in mRNA abundance across samples, and thus for each of the four mRNA expression variables (*igf1*, *igf1r*, *igf2*, and *igf2r*) we first conducted an analysis of variance (ANOVA) in PROC MIXED with tissue type as a fixed effect and individual as a random effect to quantify overall differences in mRNA abundance across tissues. We used PROC CORR to compute Pearson correlation statistics between IGF-1 and IGF-2 protein levels and between the protein levels and their respective hepatic and muscle ligand and receptor mRNA abundances.

To examine how ecotype and rearing treatment affect the IGF system, we used PROC MIXED to perform an analysis of covariance (ANCOVA) separately for the 12 different combinations of 4 genes by 3 tissue types, as well as the two protein variables (total of 14 models). Our final models included the following fixed variables: sex, ecotype, rearing treatment, ecotype × treatment, and body size at time of euthanasia (SVL). Additional interaction terms, as well as the effect of population nested within ecotype (i.e., 2 L-fast and 2 M-slow populations) were non-significant and not included in the final models. We used SVL as a covariate because it is linked to diverse physiological changes and studies have shown size effects on IGF expression irrespective of growth rates (Shimizu et al., 2009; Beckman, 2011).

To test whether recent growth affected protein and mRNA levels, we computed the change in body length from Nov. 2011 to Jan. 2012. We then used PROC CORR to compute Pearson correlation statistics between recent growth and each of the protein and mRNA variables. In all tests, significance was assessed with an α-level of 0.05.

3. Results

3.1. Data quality

Based on the presence of two clear rRNA bands in the agarose gels, and considering a 260/280 ratio of 1.8–2.2 to indicate high purity RNA free of contaminating proteins (Shipley, 2011), our methods yielded high-quality RNA. The standard curves for each of the qPCR assays were linear over the entire concentration range ($R^2 \geq 0.985$), and all Cq values of the test samples fell within the linear quantifiable range of the assays used (Table 2). The amplification efficiency estimates of the standards were similar whether derived from the slope of the dilution curve or from LinRegPCR, and were slightly higher than the efficiency estimates for the samples (Table 2). Only for IGF2 did any of the negative controls produce a positive result, at ~Cq 33.4. Visualization of the melt curve and agarose gel indicated this result was due to a small amount of primer dimer in the negative controls, which did not occur in the test samples. Furthermore, none of the test samples had Cq values >28.6, and thus could be easily distinguished from the negative controls. Standard deviations in Cq values were low among the replicates and between the positive control run on different plates (Table 2), indicating high repeatability within and among plates.

3.2. Variation in mRNA abundance across tissue type

Abundance levels of mRNA varied substantially across tissue type for all four genes (*igf1*: $F_{2,94} = 57.92$ and $P < 0.0001$; *igf1r*:

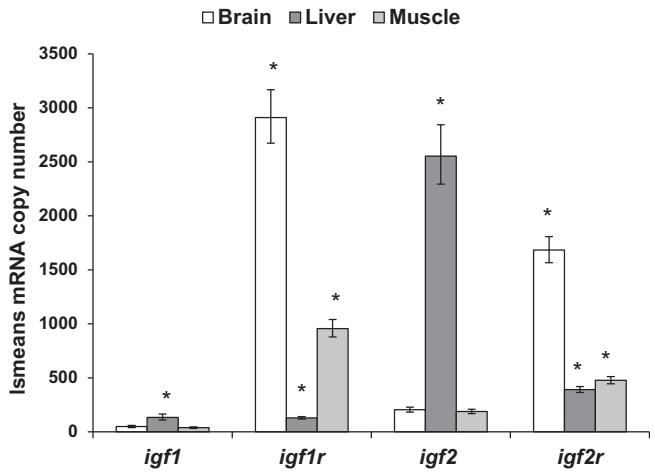

Fig. 2. Differences in mRNA abundances (back-transformed least squares means) among three tissue types (brain, liver, and skeletal muscle) for each of four genes (*igf1*, *igf1r*, *igf2*, and *igf2r*). Whiskers reflect the back-transformed upper and lower 95% confidence limits, and asterisks denote expression levels significantly different ($P < 0.05$) from expression levels in the other tissues.

Table 3
Abundance of mRNAs for *igf1*, *igf1r*, *igf2*, and *igf2r* in brain, liver, and skeletal muscle of ~1.5 year old garter snakes (back-transformed least squares means and 95% confidence intervals from mixed model ANOVA by gene).[a]

	Brain	Liver	Skeletal muscle
igf1 mRNA	48 (39–60)	134 (110–164)	38 (31–47)
igf1r mRNA	2910 (2673–3167)	129 (119–141)	956 (879–1040)
igf2 mRNA	204 (183–228)	2553 (2294–2843)	188 (168–210)
igf2r mRNA	1683 (1567–1807)	391 (365–420)	477 (445–512)

[a] Data expressed as copy number per ng total RNA.

$F_{2,93} = 1532.75$ and $P < 0.0001$; *igf2*: $F_{2,92} = 805.76$ and $P < 0.0001$; *igf2r*: $F_{2,94} = 499.04$ and $P < 0.0001$). For *igf1* and *igf2*, liver had significantly higher levels of mRNA than muscle or brain, which had comparable levels to one another (Fig. 2; Table 3). In contrast, mRNA of the receptors (*igf1r* and *igf2r*) was found in significantly higher abundance in the brain, followed by muscle, and lowest in the liver (Fig. 2; Table 3). Expression of *igf2* was consistently higher than *igf1* (Fig. 2; Table 3).

3.3. Correlations between protein levels and mRNA abundance

IGF-1 and IGF-2 plasma protein levels were only marginally correlated to one another ($r = 0.259$, $P = 0.082$). Plasma IGF-1 levels were not correlated with most mRNA levels ($P > 0.05$), but did show a negative correlation with muscle *igf1* mRNA levels ($r = -0.338$, $P = 0.022$) and brain *igf2r* levels ($r = -0.334$, $P = 0.027$). Plasma IGF-2 levels also showed no significant correlation with most mRNA levels ($P > 0.05$), except for a positive correlation with hepatic *igf2* mRNA levels ($r = 0.307$, $P = 0.032$) and muscle *igf1r* mRNA levels ($r = 0.373$; $P = 0.009$).

3.4. Effect of ecotype, treatment and other variables on body size and mRNA abundances

Body size at euthanasia, which was included as a covariate in the models for mRNA abundance and protein levels, was itself influenced by temperature. Animals in the warm treatment were significantly larger than animals in the cool treatment ($F_{1,43} = 7.99$; $P = 0.007$; Table 4) due to faster growth in the warm treatment (Fig. 3). At the time of euthanasia, animals were much smaller than size of maturation (which occurs at a minimum size

Table 4
Analysis of covariance for body size, measured as snout-vent length (SVL; mm) at time of euthanasia at approximately 1.5 years of age.

Source of variation	$F_{1,43}$	*P*	*Direction of sig. factors*
Ecotype	2.70	0.107	Na
Treatment	7.99	0.007**	Warm > Cool
Sex	2.85	0.099*	Female > Male
Ecotype × Treatment	1.23	0.273	Na
Birth SVL	9.03	0.004**	Positive

Asterisks denote marginal (*$P < 0.1$) and significant effects (**$P < 0.05$). Na = not applicable.

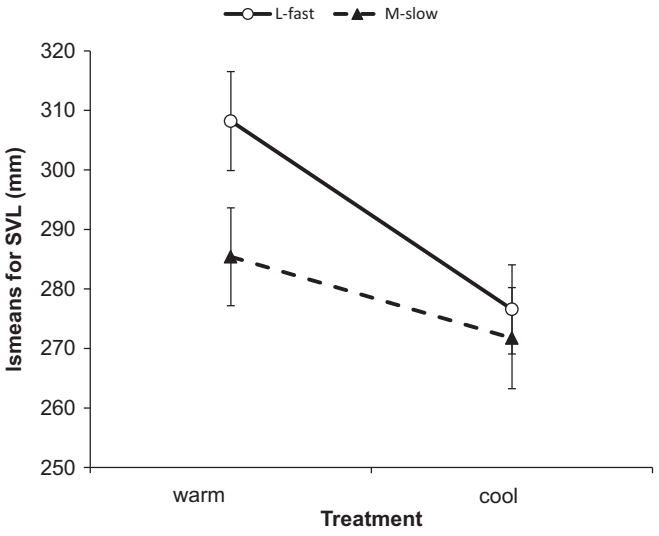

Fig. 3. Least squares means ± SEM of body size (SVL) at time of euthanasia for each of the ecotype × treatment groups, based on a model that included the following fixed effects: rearing treatment, ecotype, ecotype × treatment, sex, and birth body size. Animals in the warm treatment were significantly larger than animals in the cool treatment. Neither ecotype nor the ecotype × treatment interaction was significant.

of 400 mm SVL) and were still in the exponential phase of their growth, not yet showing slowed growth that occurs with advancing adult age in this indeterminately growing species (Bronikowski, 2000; Bronikowski and Arnold, 1999).

For *igf1*, mRNA expression in brain was significantly influenced only by sex, with males having higher levels than females (Table 5). In liver and muscle, *igf1* expression was significantly influenced by treatment, with animals in the cool treatment having higher levels (Fig. 4). Expression of muscle *igf1* showed a positive relationship to SVL, and there was a nearly significant positive relationship between liver *igf1* and SVL (Table 5).

For *igf1r*, none of the variables had a significant effect on expression levels in the brain or muscle. But in liver, L-fast animals had significantly higher mRNA abundance than M-slow (Fig. 4), warm treatment animals had significantly higher levels than cool (Fig. 4), and females had marginally higher levels than males. There was also a strong, negative relationship between liver *igf1r* expression and SVL (Table 5).

For *igf2*, none of the variables had a significant effect on brain expression levels, only SVL had a significant effect on liver expression levels (positive relationship), and treatment had a marginal effect on muscle expression levels, with cool treatment animals having slightly higher levels than the warm treatment group (Table 5; Fig. 4).

For *igf2r*, mRNA abundance in the brain was marginally affected by treatment, with the warm treatment group having slightly higher levels (Fig. 4), and significantly influenced by sex, with females having higher levels. Liver *igf2r* expression was signifi-

Table 5
Analysis of covariance (ANCOVA) for $\log_2$ mRNA levels in each of three tissues for four genes and for $\log_{10}$ protein levels in *Thamnophis elegans*.

Source of variation	IGF1 mRNA			IGF1R mRNA			IGF2 mRNA			IGF2R mRNA			Protein	
	Brain $F_{1,41}$	Liver $F_{1,43}$	Muscle $F_{1,43}$	Brain $F_{1,41}$	Liver $F_{1,43}$	Muscle $F_{1,42}$	Brain $F_{1,41}$	Liver $F_{1,43}$	Muscle $F_{1,43}$	Brain $F_{1,41}$	Liver $F_{1,43}$	Muscle $F_{1,43}$	IGF-I $F_{1,40}$	IGF-2 $F_{1,43}$
[a]Eco	1.04	0.06	0.75	1.96	15.18*** F > S	0.16	0.32	0.06	1.39	0.04	11.78*** F > S	0.13	3.29* F > S	0.17
[b]Trt	0.20	4.31** C > W	14.30*** C > W	1.42	7.34*** W > C	0.04	0.94	0.22	3.84* C > W	3.98* W > C	1.54	0.52	5.27** W > C	1.42
[c]Sex	5.15** m > f	1.23	0.68	0.08	3.79* f > m	1.41	0.03	0.07	0.00	12.46*** f > m	1.62	0.75	9.99*** m > f	10.12*** m > f
[d]SVL	0.07	3.91* (+)	11.09*** (+)	2.23	24.82*** (−)	0.00	0.38	4.21** (+)	1.29	1.17	4.73** (−)	2.76	0.45	0.77
Eco × Trt	0.19	0.22	0.30	0.87	1.88	0.06	1.28	0.88	0.08	0.98	0.00	0.44 FW, FC, SW > SC	3.10*	0.31

Asterisks denote marginal ($^{*}P < 0.1$) and significant effects ($^{**}P < 0.05$; $^{***}P < 0.01$).
[a] F = L-fast ecotype; S = M-slow ecotype.
[b] C = cool treatment; W = warm treatment.
[c] m = male; f = female.
[d] (+) = positive relationship; (−) = negative relationship.

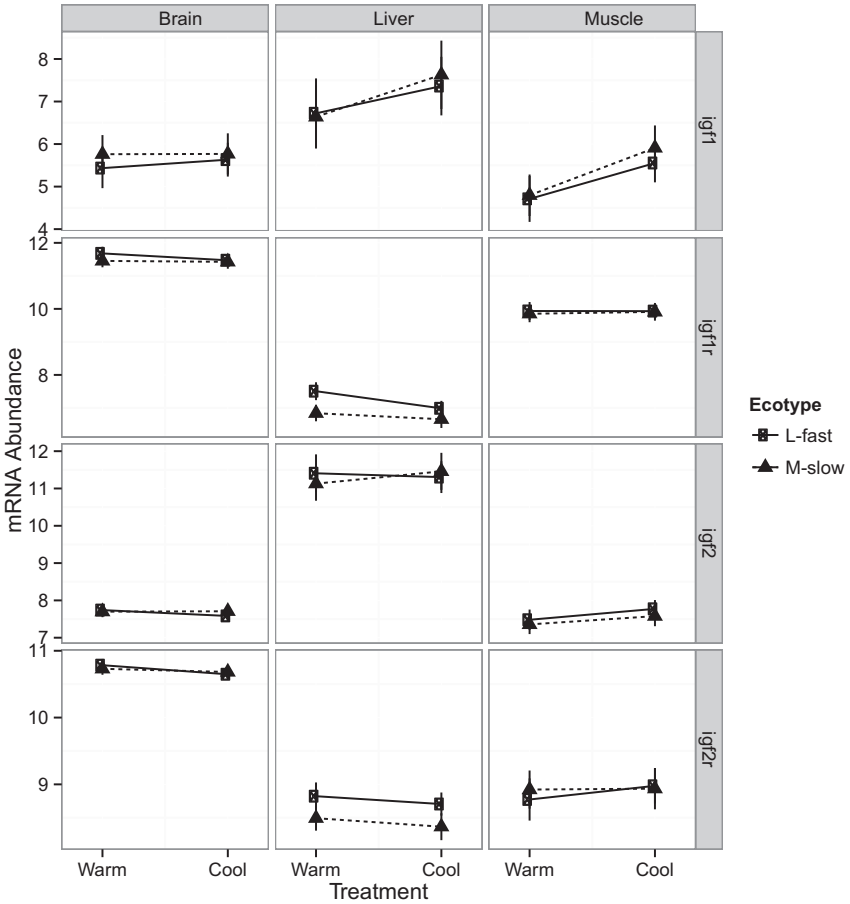

Fig. 4. Least squares means ± 95% confidence limits of mRNA abundance ($\log_2$ copy number per ng total RNA) for each of the four ecotype × rearing treatment groups across the four genes and 3 tissue types. Note that the scale of the Y-axis differs among the genes.

cantly higher in L-fast animals, and there was a significant, negative relationship between liver *igf2r* and SVL. None of the variables were significantly related to *igf2r* expression in muscle (Table 5).

3.5. Effect of treatment, ecotype and other variables on protein levels

Circulating IGF-1 protein levels were marginally influenced by the ecotype × treatment interaction (Table 5). This result is driven by significantly lower IGF-1 levels in M-slow animals in the cool treatment than in any of the other 3 groups (Fig. 5; Table 5). Circulating IGF-1 protein levels were also significantly influenced by sex, with males having higher levels than females (Table 5). Circulating IGF-2 protein levels were only influenced by sex, with males showing significantly higher levels than females (Table 5).

3.6. Correlations between recent growth and mRNA and protein levels

Individual growth rate varied among individuals in the two months prior to our terminal measures (mean mm ± SD: Warm L-fast = 9.8 ± 7.4; Cool L-fast = 11.7 ± 7.1; Warm M-slow = 7.3 ±

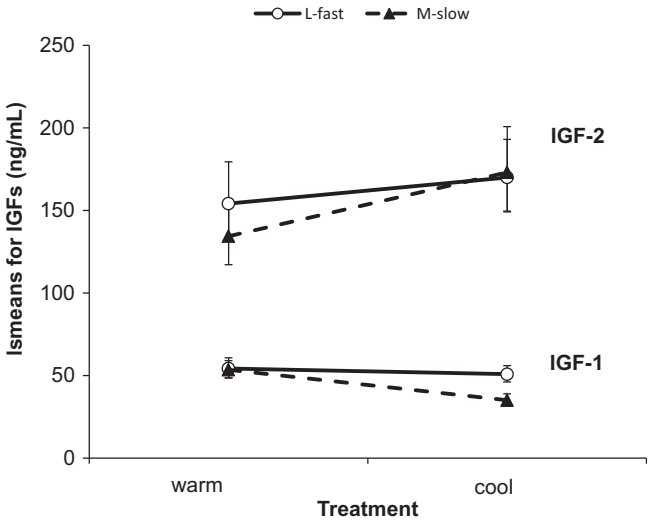

Fig. 5. Differences in circulating IGF protein levels (back-transformed least squares means ± SEM) for each of the ecotype × treatment groups, based on a model that included the following fixed effects: rearing treatment, ecotype, ecotype × treatment, and sex.

4.5; Cool M-slow = 15.4 ± 10.2). In our test for how this growth rate variation affected IIS variables, we found that plasma IGF-1 levels were negatively correlated with recent growth (r = -0.583, P < 0.0001; Fig. 6a), whereas IGF-2 levels showed no significant relationship to recent growth (r = −0.221, P = 0.127). No correlations were observed between recent growth and hepatic *igf1* and *igf2* levels (P > 0.05). However, positive correlations were observed between recent growth and muscle mRNA levels of *igf1* (r = 0.538, P < 0.001; Fig. 6b) and *igf2* (r = 0.377, P = 0.009; Fig. 6c).

4. Discussion

Much of our understanding of IGF structure, function, and regulation comes from research on mammalian systems, for which IGF-1 in particular has been shown to exert diverse and pleiotropic influences on fundamental physiological functions related to life history characteristics. For example, IGF-1 signaling promotes embryonic and postnatal growth and development (Baker et al., 1993; Stratikopoulos et al., 2008) and increases reproduction via larger litter sizes and/or early maturation (Gay et al., 1997; Hiney et al., 1996), but decreases longevity (Holzenberger et al., 2003; Kappeler et al., 2008). In contrast, IGF-2 is thought to primarily function at prenatal stages by regulating placental and fetal growth and development (Constancia et al., 2002). However, the biological role of IGF-2 and its potential overlap in function with IGF-1 is far from clear, even in well-studied mammals (Holly, 1998; Wolf et al., 1998; Brown et al., 2009). Considerable variation in postnatal IGF-2 levels has been observed among species. For example, IGF-2 is virtually absent after birth in rodents but is the most abundant circulating IGF in juvenile and adult humans (LeRoith and Roberts, 2003; but see Qiu et al., 2007). The picture is even more complicated when studies from non-mammalian vertebrates are considered. Systemic IGF-2 appears to be postnatally expressed in ectothermic reptiles, as McGaugh et al. (2015) detected *igf2* mRNA in the liver transcriptomes of 17 diverse reptile species examined. Some studies in fish (Peterson et al., 2004) and birds (Beccavin et al., 2001) have even found higher hepatic mRNA expression levels or circulating protein levels of IGF-2 than IGF-1 in juveniles. Furthermore, studies in some teleost fish have found not only high postnatal expression of IGF-2, but also that expression levels respond to nutritional status and correlate with growth rates

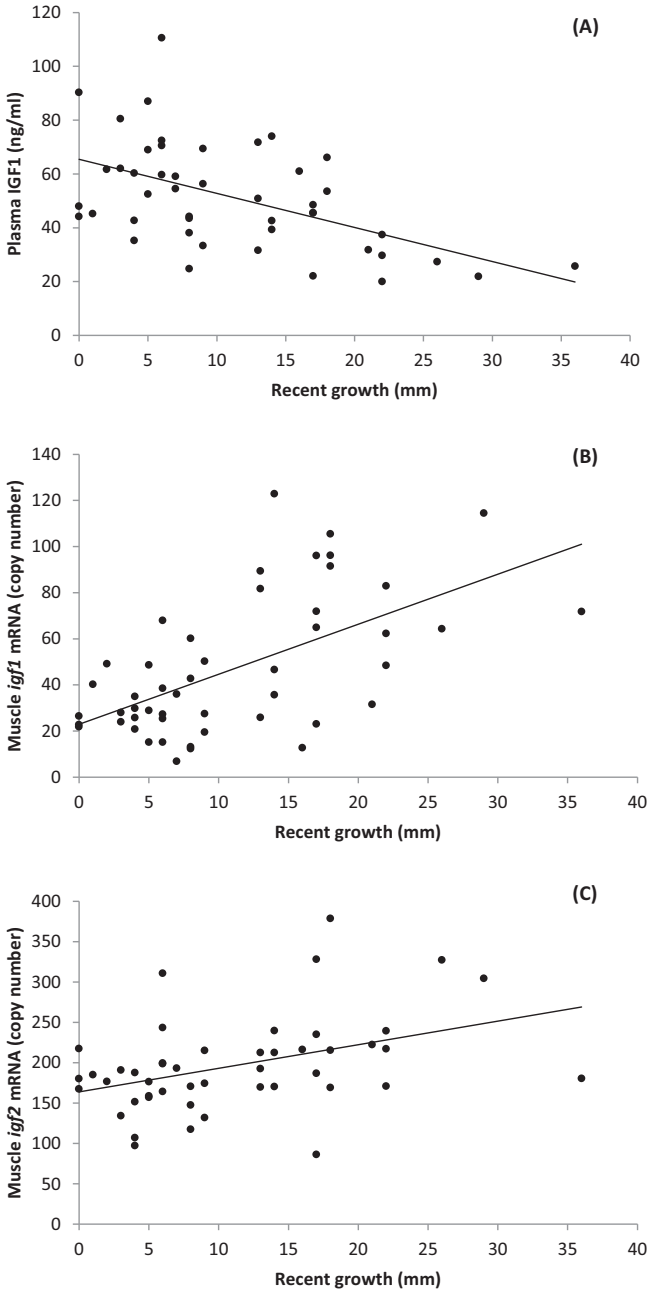

Fig. 6. Relationship between recent growth (change in SVL from Nov. 2011 to Jan. 2012) in juvenile *T. elegans* and (a) plasma IGF-1 levels; (b) *igf1* mRNA abundance in skeletal muscle; and (c) *igf2* mRNA abundance in skeletal muscle.

(Wood et al., 2005; Picha et al., 2008; Pierce et al., 2011). Thus, IGF-2 may contribute substantially to the regulation of postnatal growth and development, particularly in non-mammalian vertebrate species.

Previous work in non-avian reptiles has detected: (1) IGF-1 in the plasma of juvenile and/or adult lizards (Duncan et al., 2015), snakes (Sparkman et al., 2009, 2010), turtles (Crain et al., 1995a, b; Daughaday et al., 1985), and alligators (Crain et al., 1995b; Guillette et al., 1996); (2) IGF-2 in the plasma of turtles (Daughaday et al., 1985) and adult snakes (E. A. Addis and A. M. Bronikowski, unpublished data); (3) IGF-1 and IGF-2 in skeletal tissues of lizards (Bautista et al., 1990); (4) IGF-1 and IGF-2 in the pancreas of lizards and snakes (Reinecke et al., 1995); IGF1R in the brain of lizards (Shemer et al., 1987); IGF2R in the liver of

lizards (Yadavalli et al., 2009); (5) mRNA expression of *igf1*, *igf2*, *igf1r*, and *igf2r* in the liver of 17 species of reptiles representing turtles, lizards, snakes, and alligators (McGaugh et al., 2015); and (6) rapid divergence in IGF-1 coding sequence among lizards and snakes (Sparkman et al., 2012). Here, we add to this limited knowledge of the IGF system in non-avian reptiles.

4.1. mRNA expression and plasma protein levels

We detected both IGF-1 and IGF-2 plasma proteins, and we detected *igf1*, *igf2*, *igf1r* and *igf2r* transcripts in all three of the tissue types examined. The overall pattern of mRNA expression in this system indicates that genes for the IGF ligands are more highly expressed in the liver than in other tissues such as brain and skeletal muscle. These findings are consistent with the general conclusion that, although expressed in most tissue types, the liver is the primary site of IGF transcription in vertebrates (Reindl and Sheridan, 2012). We also found that the brain had the highest expression levels of the IGF receptors. Based on mammalian models, these receptors may be exposed to IGF ligands produced locally and/or circulating IGFs transported across the blood brain barrier, depending on the brain region involved (Fernandez and Torres-Alemán, 2012). Thus, future work to identify the cellular localization of IGFs and receptors in the brain of reptiles would be beneficial to understanding how different regions facilitate or respond to IGF signaling.

Owing to high mRNA expression, in turn, the liver is thought to be the main source of endocrine (i.e., circulating in the blood) IGF-1 and IGF-2 peptides (Le Roith et al., 2001). Indeed, numerous studies have found strong, positive correlations between hepatic mRNA expression and plasma protein levels (e.g., Pierce et al., 2005; Picha et al., 2008). Although we found a significant positive correlation between hepatic mRNA and plasma protein levels for IGF-2, this was not the case for IGF-1. This result may be indicative of an alternative endocrine source for IGF-1. However, we did not observe a positive correlation between plasma IGF-1 levels and muscle *igf1* expression; in fact, we observed a significant *negative* correlation between plasma IGF-1 and muscle *igf1* suggestive of a negative feedback mechanism between endocrine protein levels and local transcription rates. Although our findings do not preclude the possibility of contributions to plasma IGF-1 from other extra-hepatic tissues that we did not sample (Reinecke, 2010), there is a general lack of evidence to support a source of endocrine IGF-1 other than liver and possibly skeletal muscle (Stratikopoulos et al., 2008).

Opposite to the prediction based on mammalian systems, we found reptilian postnatal expression of *igf2* at levels substantially higher than *igf1* in liver (19.1-fold), brain (4.3-fold), and skeletal muscle (4.9-fold). Furthermore, our overall untransformed mean for circulating IGF-2 protein levels in *T. elegans* (173 ng/mL) was likely higher than IGF-1 (51 ng/mL), though the heterologous RIA used here warrants caution when comparing the two protein levels. Although these findings are contradictory to expectations based on mammalian model systems, in which IGF-2 expression generally declines and postnatal growth is primarily controlled by GH-regulated expression of IGF-1, some studies in other vertebrates have found results similar to ours. For example, Peterson et al. (2004) found that *igf2* mRNA levels were higher than *igf1* in both liver (5.8-fold) and muscle (12.2-fold) of channel catfish. Daughaday et al. (1985) detected higher levels of IGF-2 (100 ng/mL) than IGF-1 (17 ng/mL) in the sera of juvenile turtles, as did Beccavin et al. (2001) in post-hatch chickens.

Indeed, a growing body of research suggests that IGF-2 abundance, function, and regulation may differ between placental and non-placental vertebrates. Studies indicate that mammals exhibit up to 100 times more IGF-1 in their blood than non-mammals (Kelley et al., 2002) and that IGF-2 is abundantly expressed in juvenile and adult teleost fish (Peterson et al., 2004; Wood et al., 2005; Picha et al., 2008; Pierce et al., 2011) and reptiles (McGaugh et al., 2015), but nearly absent in rodents (Holly and Perks, 2012). Furthermore, studies in some teleost fish species indicate that liver *igf2* expression and plasma levels are stimulated by growth hormone (GH; Vong et al., 2003; Pierce et al., 2010) and in some cases respond to metabolic status to a greater degree than IGF-1 (Pierce et al., 2011). In garter snakes, liver expression of *igf2* decreases in response to a 2-h heat stress treatment (Schwartz and Bronikowski, 2014), further suggesting that its expression is responsive to the immediate environmental conditions. Although affinity of IGF1R for IGF-1 is typically greater than IGF-2 in mammals, Pozios et al. (2001) found similar affinities in zebrafish. Finally, evolutionary analysis of insulin-like signaling gene sequences across amniotes indicates that *igf2* may have a more stable role in environmental-sensing and growth-signaling in reptiles than does *igf1*, which has this function in mammals (McGaugh et al., 2015). Thus, an understanding of the IGFs system based on mammalian model systems may not be applicable to fish, reptiles, and other vertebrate groups.

4.2. Treatment and ecotype

Based on an understanding of the IGFs system from lab model, commercial, and wild organisms and the life history characteristics of *T. elegans*, we predicted that the genetic background characterized by slow juvenile growth (M-slow) and cool treatment animals would exhibit lower IGF-1 and IGF-2 protein levels and lower *igf1*, *igf1r*, and *igf2* mRNA levels than the L-fast and warm treatment animals. Limited data from reptiles also support these predictions, as hepatic *igf1* mRNA and plasma IGF-1 levels were reduced in lizards under food restriction (Duncan et al., 2015), plasma IGF-1 levels were higher in wild-caught fast-growing L-fast *T. elegans* than slow-growing M-slow snakes (Sparkman et al., 2009), and turtles with a higher protein and energy diet showed elevated levels of plasma IGF-1 (Crain et al., 1995b).

We found mixed support for these predictions. For example, IGF-1 protein levels were significantly lower in M-slow, cool treatment animals, and liver *igf1r* mRNA levels were higher in L-fast and warm treatment animals. However, opposite to our expectations, we found that muscle and liver *igf1* and *igf2* mRNA levels were higher in the cool than warm treatment, and liver *igf2r* mRNA levels were higher in the L-fast than M-slow animals. Part of the incongruity with our predictions can likely be attributed to the fact that, although warm treatment animals exhibited more growth overall (see Fig. 3; see also Gangloff et al., 2015; E.A. Addis and A.M. Bronikowski, unpublished data), during this short duration immediately preceding our sampling, the cool treatment animals grew faster (see Section 3.6).

Another challenge in interpreting these results is that nutritional status can produce not only acute effects on IGF levels, but also long-term effects that may be opposite to the observed short-term effects (Holly and Perks, 2012). To better understand this relationship, data for growth, nutrition, and IGFs collected over multiple time points would be helpful. Relating to the potential long-term programming effects of nutrition on IGFs action, another helpful piece of information would be the extent of variability in maternal nutrient availability during gestation, as recent studies have shown that maternal nutrition can have long-term effects on offspring. For example, Micke et al. (2011) found that maternal protein restriction during the first trimester in cattle affected postnatal skeletal muscle growth and *igf1*, *igf1r*, *igf2*, *igf2r* mRNA expression in mature offspring, with observed sex-specific effects. Since we captured gravid females from the wild, maternal nutritional information during early gestation was not available for this experiment.

4.3. IGF signaling and postnatal growth

In this experiment, the environment (rearing treatment) significantly influenced overall growth (increase in length) of juvenile snakes, whereas genetic backgroud (ecotype) had a minor effect with L-fast animals tending to grow more than M-slow (see Section 3.4; E.A. Addis and A.M. Bronikowski, unpublished data). Many studies report a positive relationship between postnatal growth rate, energy intake, and systemic IGF-1 levels (e.g., Sparkman et al., 2010; Lodjak et al., 2014). Overall, our warm treatment animals consumed more food (Gangloff et al., 2015), exhibited more growth (E.A. Addis and A.M. Bronikowski, unpublished data), and had higher plasma IGF-1 levels than the cool treatment group. Considering the intra-individual correlations between growth and our IIS measures, IGF-1 decreased with increasing growth rates, whereas muscle *igf1* and *igf2* increased with increasing growth rates. It is unclear whether IGF-1 plasma levels are more indicative of future or past growth events, though Beckman et al. (2004) found that the tightest positive relationship between IGF-1 and growth in fish occurred within the month prior to sampling. Furthermore, in addition to systemic IGF1, local production of this protein in tissues such as skeletal muscle may act in a paracrine/autocrine fashion to stimulate tissue growth (Chauvigné et al., 2003; Eppler et al., 2007). For example, a study by Eppler et al. (2007) highlights the potential importance of locally produced IGF-1, as transgenic tilapia with increased growth showed higher skeletal *igf1* mRNA expression, but lower plasma IGF-1. In non-mammalian vertebrates, systemic and local IGF-2 may also act as a mitogen in postnatal life, which may be a factor in this experiment given the high expression and plasma levels of this protein. Finally, the role of sequence variation in the IGF genes needs to be explored, as recent evidence indicates that the presence or absence of a single *IGF1* nucleotide polymorphism may determine body size in dogs (Sutter et al., 2007) and thus potentially other species.

5. Conclusions

Based on accumulating evidence from laboratory and domestic animals, the IIS pathway regulates growth, reproduction, lifespan and other key life history traits. Although some common patterns regarding the relationship between IGF activity and life history traits such as growth rate have emerged from studies of mammalian species, research on non-mammalian vertebrates from natural populations is limited. Here we report on the complex relationship between IGFs (mRNA and protein), postnatal growth, and the environmental and genetic variation that contribute to ecotypic differences in life history in garter snakes. One key finding is that although both *igf1* and *igf2* were expressed in liver, skeletal muscle, and brain tissue, *igf2* mRNA and protein levels were substantially higher than *igf1* in this reptile, and cool treatment animals (which grew more in the preceding two months) demonstrated significantly higher *igf2* as well as *igf1* expression in skeletal muscle. Thus, this study adds to a small but growing body of literature indicating that *igf2* may play a more evolutionarily stable and prominent role in postnatal growth and environmental sensing in non-placental vertebrates, whereas *igf1* primarily encompasses this role in placental mammals. A second major outcome of this study is that rearing temperature treatment had a more substantial impact on growth and IGF activity than ecotype, and for the most part the two ecotypes responded similarly (i.e., no G × E interaction). These results suggest that observed ecotypic differences in field measures of IGFs may more strongly reflect plastic responses in different environments than adaptive genetic divergence. However, future studies should investigate potential sequence differences among the ecotypes for these four genes, as well as other components of the IIS pathway, in order to further tease apart the relative contributions of environmental and genetic factors in shaping these divergent life history strategies in *T. elegans*.

Acknowledgments

This research was supported by a grant from the National Science Foundation to AMB (IOS-0922528), and a grant from the Iowa State University Center for Integrated Animal Genomics to AMB. E. Addis was supported by a science education research fellowship provided by the Howard Hughes Medical Institute. We thank Kirsten Hofmockel for access to laboratory equipment for performing qPCR, Jack Gallup for advice and feedback on qPCR efficiency and copy number calculations, and Carol Vleck for laboratory space and advice on performing radioimmunoassays.

Appendix A. Supplementary data

Supplementary data associated with this article can be found, in the online version, at http://dx.doi.org/10.1016/j.ygcen.2016.05.018.

References

Annunziata, M., Granata, R., Ghigo, E., 2011. The IGF system. Acta Diabetol. 48, 1–9.
Baker, J., Liu, J.P., Robertson, E.J., Efstratiadis, A., 1993. Role of insulin-like growth factors in embryonic and postnatal growth. Cell 75, 73–82.
Bartke, A., 2005. Minireview: role of the growth hormone/insulin-like growth factor system in mammalian aging. Endocrinology 146, 3718–3723.
Bautista, C.M., Mohan, S., Baylink, D.J., 1990. Insulin-like growth factors I and II are present in the skeletal tissues of ten vertebrates. Metabolism 39, 96–100.
Beccavin, C., Chevalier, B., Cogburn, L., Simon, J., Duclos, M., 2001. Insulin-like growth factors and body growth in chickens divergently selected for high or low growth rate. J. Endocrinol. 168, 297–306.
Beckman, B.R., 2011. Perspectives on concordant and discordant relations between insulin-like growth factor 1 (IGF1) and growth in fishes. Gen. Comp. Endocrinol. 170, 233–252.
Beckman, B.R., Shimizu, M., Gadberry, B.A., Cooper, K.A., 2004. Response of the somatotropic axis of juvenile coho salmon to alterations in plane of nutrition with an analysis of the relationships among growth rate and circulating IGF-I and 41 kDa IGFBP. Gen. Comp. Endocrinol. 135, 334–344.
Bronikowski, A.M., 2000. Experimental evidence for the adaptive evolution of growth rate in the garter snake (*Thamnophis elegans*). Evolution 54, 1760–1767.
Bronikowski, A.M., Arnold, S.J., 1999. The evolutionary ecology of life history variation in the garter snake *Thamnophis elegans*. Ecology 80, 2314–2325.
Brown, J., Jones, E.Y., Forbes, B.E., 2009. Keeping IGF-II under control: lessons from the IGF-II-IGF2R crystal structure. Trends Biochem. Sci. 34, 612–619.
Charnov, E.L., 1993. Life History Invariants: Some Explorations of Symmetry in Evolutionary Ecology. Oxford University Press, Oxford.
Chauvigné, F., Gabillard, J.C., Weil, C., Rescan, P.Y., 2003. Effect of refeeding on IGFI, IGFII, IGF receptors, FGF2, FGF6, and myostatin mRNA expression in rainbow trout myotomal muscle. Gen. Comp. Endocrinol. 132, 209–215.
Clemmons, D.R., 2003. IGF binding proteins and their functions. Mol. Reprod. Dev. 35, 368–375.
Constancia, M. et al., 2002. Placental-specific IGF-II is a major modulator of placental and fetal growth. Nature 417, 945–948.
Crain, D.A., Bolten, A.B., Bjorndal, K.A., Guillette, J.L.J., Gross, T.S., 1995a. Size-dependent, sex-dependent, and seasonal changes in insulin-like growth factor I in the loggerhead sea turtle (*Caretta caretta*). J. Endocrinol. 98, 219–226.
Crain, D.A., Gross, T.S., Cox, C., Guillette, J.L.J., 1995b. Insulin-like growth factor-I in the plasma of two reptiles: assay development and validations. Gen. Comp. Endocrinol. 98, 26–34.
D'Ercole, A.J., Stiles, A.D., Underwood, L.E., 1984. Tissue concentrations of somatomedin-C: further evidence for multiple sites of synthesis and paracrine or autocrine mechanisms of action. Proc. Natl. Acad. Sci. U.S.A. 81, 935–939.
Dantzer, B., Swanson, E.M., 2012. Mediation of vertebrate life histories *via* insulin-like growth factor-1. Biol. Rev. Camb. Philos. Soc. 87, 414–429.
Daughaday, W.H., Kapadia, M., Yanow, C.E., Fabrick, K., Mariz, I.K., 1985. Insulin-like growth factors I and II of nonmammalian sera. Gen. Comp. Endocrinol. 59, 316–325.
Denley, A., Cosgrove, L.J., Booker, G.W., Wallace, J.C., Forbes, B.E., 2005. Molecular interactions of the IGF system. Cytokine Growth Factor Rev. 16, 421–439.
Duncan, C.A., Jetzt, A.E., Cohick, W.S., John-Alder, H.B., 2015. Nutritional modulation of IGF-1 in relation to growth and body condition in Sceloporus lizards. Gen. Comp. Endocrinol. 216, 116–124.

El-Shewy, H.M., Lee, M.H., Obeid, L.M., Jaffa, A.A., Luttrell, L.M., 2007. The insulin like growth factor type 1 and insulin-like growth factor type 2/mannose-6-phosphate receptors independently regulate ERK1/2 activity in HEK293 cells. J. Biol. Chem. 282, 26150–26157.
Eppler, E., Caelers, A., Shved, N., Hwang, G., Rahman, A.M., Maclean, N., Zapf, J., Reinecke, M., 2007. Insulin-like growth factor I (IGF-I) in a growth-enhanced transgenic (GH-overexpressing) bony fish, the tilapia (*Oreochromis niloticus*): indication for a higher impact of autocrine/paracrine than of endocrine IGF-I. Transgenic Res. 16, 479–489.
Ewton, D.Z., Falen, S.L., Florini, J.R., 1987. The type II insulin-like growth factor (IGF) receptor has low affinity for IGF-I analogs: pleiotypic actions of IGFs on myoblasts are apparently mediated by the type I receptor. Endocrinology 120, 115–123.
Fernandez, A.M., Torres-Alemán, I., 2012. The many faces of insulin-like peptide signaling in the brain. Nat. Rev. Neurosci. 13, 225–239.
Flatt, T., Heyland, A., 2011. Mechanisms of Life History Evolution: The Genetics and Physiology of Life History Traits and Trade-Offs. Oxford University Press, Oxford.
Gallup, J.M., 2011. QPCR inhibition and amplification of difficult templates. In: Kennedy, S., Oswald, N. (Eds.), PCR Troubleshooting and Optimization: The Essential Guide. Caister Academic Press, Norfolk, UK, pp. 23–65.
Gangloff, E.J., Vleck, D., Bronikowski, A.M., 2015. Developmental and immediate thermal environments shape energetic trade-offs, growth efficiency, and metabolic rate in divergent life-history ecotypes of the garter snake *Thamnophis elegans*. Physiol. Biochem. Zool. 88.
Gay, E., Seurin, D., Babajko, S., Doublier, S., Cazillis, M., Binoux, M., 1997. Liver-specific expression of human insulin-like growth factor binding protein-1 in transgenic mice: repercussions on reproduction, ante- and perinatal mortality and postnatal growth. Endocrinology 138, 2937–2947.
Guillette, L.J., Cox, M.C., Crain, D.A., 1996. Plasma insulin-like growth factor-1 concentration during the reproductive cycle of the American alligator (*Alligator mississippiensis*). Gen. Comp. Endocrinol. 104, 116–122.
Hiney, J.K., Srivastava, V., Nyberg, C.L., Ojeda, S.R., Dees, W.L., 1996. Insulin-like growth factor I of peripheral origin acts centrally to accelerate the initiation of female puberty. Endocrinology 137, 3717–3728.
Holly, J.M.P., 1998. The IGF-II enigma. Growth Horm. IGF Res. 8, 183–184.
Holly, J.M.P., Perks, C.M., 2012. Insulin-like growth factor physiology: what we have learned from human studies. Endorinol. Metab. Clin. North Am. 41, 249–263.
Holzenberger, M., Dupont, J., Ducos, B., Leneuve, P., Geloen, A., Even, P.C., Cervera, P., Le Bouc, Y., 2003. IGF-1 receptor regulates lifespan and resistance to oxidative stress in mice. Nature 421, 182–187.
Hou, Y., Zhang, H., Miranda, L., Lin, S., 2010. Serious overestimation in quantitative PCR by circular (supercoiled) plasmid standard: microalgal *pcna* as the model gene. PLoS One 5, e9545.
Huey, R.B., Peterson, C.R., Arnold, S.J., Porter, W.P., 1989. Hot rocks and not-so-hot rocks: Retreat-site selection by garter snakes and its thermal consequences. Ecology 70, 931–944.
Kappeler, L., Filho, C.D.M., Dupont, J., Leneuve, P., Cervera, P., Perin, L., Loudes, C., Blaise, A., Klein, R., Epelbaum, J., Le Bouc, Y., Holzenberger, M., 2008. Brain IGF-1 receptors control mammalian growth and lifespan through a neuroendocrine mechanism. PLoS Biol. 6, 2144–2153.
Kavanagh, I., Jones, G., Nayab, S.N., 2011. Significance of controls and standard curves in PCR. In: Kennedy, S., Oswald, N. (Eds.), PCR Troubleshooting and Optimization: The Essential Guide. Caister Academic Press, Norfolk, UK, pp. 67–78.
Kelley, K.M., Schmidt, K.E., Berg, L., Sak, K., Galima, M.M., Gillespie, C., Balogh, L., Hawayek, A., Reyes, J.A., Jamison, M., 2002. Comparative endocrinology of the insulin-like growth factor-binding protein. J. Endocrinol. 175, 3–18.
Ketterson, E.D., Nolan, V., 1992. Hormones and life histories – an integrative approach. Am. Nat. 140, S33–S62.
Le Roith, D., Bondy, C., Yakar, S., Liu, J.L., Butler, A., 2001. The somatomedin hypothesis: 2001. Endocr. Rev. 22, 53–74.
LeRoith, D., Roberts Jr., C.T., 2003. The insulin-like growth factor system and cancer. Cancer Lett. 195, 127–137.
Lodjak, J., Mägi, M., Tilgar, V., 2014. Insulin-like growth factor 1 and growth rate in nestlings of a wild passerine bird. Funct. Ecol. 28, 159–166.
McGaugh, S.E., Bronikowski, A.M., Kuo, C., Reding, D.M., Addis, E.A., Flagel, L.E., Janzen, F.J., Schwartz, T.S., 2015. Rapid molecular evolution across amniotes of the IIS/TOR network. Proc. Natl. Acad. Sci. U.S.A. 112, 7055–7060.
Micke, G.C., Sullivan, T.M., McMillen, I.C., Gentili, S., Perry, V.E.A., 2011. Protein intake during gestation affects postnatal bovine skeletal muscle growth and relative expression of IGF1, IGF1R, IGF2, and IGF2R. Mol. Cell. Endocrinol. 332, 234–241.
Miller, D.A., Clark, W.R., Arnold, S.J., Bronikowski, A.M., 2011. Stochastic population dynamics in populations of western terrestrial garter snakes with divergent life histories. Ecology 92, 1658–1671.
Nakae, J., Kido, Y., Accili, D., 2001. Distinct and overlapping functions of insulin and IGF-I receptors. Endocr. Rev. 22, 818–835.
Orr, M.R., Smith, T.B., 1998. Ecology and speciation. Trends Ecol. Evol. 13, 502–506.
Peterson, C.R., Gibson, A.R., Dorcas, M.E., 1993. Snake thermal ecology: the causes and consequences of body-temperature variation. In: Seigel, R.A., Collins, J.T. (Eds.), Snakes: Ecology and Behavior. McGraw-Hill, New York, pp. 241–314.
Peterson, B.C., Waldbieser, G.C., Bilodeau, L., 2004. IGF-I and IGF-II mRNA expression in slow and fast growing families of USDA103 channel catfish (*Ictalurus punctuatus*). Comp. Biochem. Physiol. Part A 139, 317–323.
Pfaffl, M.W., 2004. Quantification strategies in real-time PCR. In: Bustin, S.A. (Ed.), A-Z of Quantitative PCR. International University Line, La Jolla, CA, pp. 87–112.
Picha, M.E., Turano, M.J., Tipsmark, C.K., Borski, R.J., 2008. Regulation of endocrine and paracrine sources of Igfs and Gh receptor during compensatory growth in hybrid striped bass (*Morone chrysops* × *Morone saxatilis*). J. Endocrinol. 199, 81–94.
Pierce, A.L., Shimizu, M., Beckman, B.R., Baker, D.M., Dickhoff, W.W., 2005. Time course of the GH/IGF axis response to fasting and increased ration in chinook salmon (*Oncorhynchus tshawytscha*). Gen. Comp. Endocrinol. 140, 192–202.
Pierce, A.L., Dickey, J.T., Felli, L., Swanson, P., Dickhoff, W.W., 2010. Metabolic hormones regulate basal and growth hormone-dependent *igf2* mRNA in primary cultured coho salmon hepatocytes: effects of insulin, glucagon, dexamethasone, and triiodothyronine. J. Endocrinol. 204, 331–339.
Pierce, A.L., Breves, J.P., Moriyama, S., Hirano, T., Grau, E.G., 2011. Differential regulation of Igf1 and Igf2 mRNA levels in tilapia hepatocytes: effects of insulin and cortisol on GH sensitivity. J. Endocrinol. 211, 201–210.
Pozios, K.C., Ding, J., Degger, B., Upton, Z., Duan, C., 2001. IGFs stimulate zebrafish cell proliferation by activating MAP kinase and PI3-kinase-signaling pathways. Am. J. Physiol. Regul. Integr. Comp. Physiol. 280, R1230–R1239.
Promislow, D.E.L., Harvey, P.H., 1990. Living fast and dying young: a comparative analysis of life history variation among mammals. J. Zool. 220, 417–437.
Qiu, Q., Jiang, J.Y., Bell, M., Tsang, B.K., Gruslin, A., 2007. Activation of endoproteolytic processing of insulin-like growth factor-II in fetal, early postnatal, and pregnant rats and persistence of circulating levels in postnatal life. Endocrinology 148, 4803–4811.
Ramakers, C., Ruijter, J.M., Lekanne Deprez, R.H., Moorman, A.F.M., 2003. Assumption-free analysis of quantitative real-time polymerase chain reaction (PCR) data. Neurosci. Lett. 339, 62–66.
Reindl, K.M., Sheridan, M.A., 2012. Peripheral regulation of the growth hormone-insulin-like growth factor system in fish and other vertebrates. Comp. Biochem. Physiol. Part A 163, 231–245.
Reinecke, M., 2010. Influences of the environment on the endocrine and paracrine fish growth hormone-insulin-like growth factor-I system. J. Fish Biol. 76, 1233–1254.
Reinecke, M., Broger, I., Brun, R., Zapf, J., Maake, C., 1995. Innunohistochemical localization of insulin-like growth factor I and II in the endocrine pancreas of birds, reptiles, and amphibia. Gen. Comp. Endocrinol. 100, 385–396.
Ricklefs, R.E., 2000. Density dependence, evolutionary optimization, and the diversification of avian life histories. Condor 102, 9–22.
Ricklefs, R.E., Wikelski, M., 2002. The physiology/life history nexus. Trends Ecol. Evol. 17, 462–468.
Ruijter, J.M., Ramakers, C., Hoogaars, et al., 2009. Amplification efficiency: linking baseline and bias in the analysis of quantitative PCR data. Nucleic Acids Res. 37 e45.
Rundle, H.D., Nosil, P., 2005. Ecological speciation. Ecol. Lett. 8, 336–352.
Schluter, D., 2001. Ecology and the origin of species. Trends Ecol. Evol. 16, 372–380.
Schrader, M., Travis, J., 2012. Embryonic IGF2 expression is not associated with offspring size among populations of a placental fish. PLoS One 7, e45463.
Schwartz, T.S., Bronikowski, A.M., 2011. Molecular stress pathways and the evolution of life histories in reptiles. In: Flatt, T., Heyland, A. (Eds.), Mechanisms of Life History Evolution: The Genetics and Physiology of Life History Traits and Trade-Offs. Oxford University Press, Oxford, pp. 193–209.
Schwartz, T.S., Bronikowski, A.M., 2013. Dissecting molecular stress networks: identifying nodes of divergence between life-history phenotypes. Mol. Ecol. 22, 739–756.
Schwartz, T.S., Bronikowski, A.M., 2014. Gene expression of components of the insulin/insulin-like signaling pathway in response to heat stress in the garter snake, *Thamnophis elegans*. J. Iowa Acad. Sci. 121 (1–4), 1–4.
Schwartz, T.S., Tae, H., Yang, Y., Mockaitis, K., Van Hemert, J.L., Proulx, S.R., Choi, J., Bronikowski, A.M., 2010. A garter snake transcriptome: pyrosequencing, de novo assembly, and sex-specific differences. BMC Genomics 11, 694.
Shemer, J., Raizada, M.K., Masters, B.A., Ota, A., LeRoith, D., 1987. Insulin-like growth factor I receptors in neuronal and glial cells. Characterization and biological effects in primary culture. J. Biol. Chem. 262, 7693–7699.
Shimizu, M., Cooper, K.A., Dickhoff, W.W., Beckman, B.R., 2009. Postprandial changes in plasma growth hormone, insulin, insulin-like growth factor (IGF)-I, and IGF-binding proteins in coho salmon fasted for varying periods. Am. J. Physiol. 297, R352–R361.
Shipley, G., 2011. The MIQE guidelines uncloaked. In: Kennedy, S., Oswald, N. (Eds.), PCR Troubleshooting and Optimization: The Essential Guide. Caister Academic Press, Norfolk, UK, pp. 151–165.
Sparkman, A.M., Vleck, C.M., Bronikowski, A.M., 2009. Evolutionary ecology of endocrine-mediated life-history variation in the garter snake *Thamnophis elegans*. Ecology 90, 720–728.
Sparkman, A.M., Byars, D., Ford, N.B., Bronikowski, A.M., 2010. The role of insulin-like growth factor-1 (IGF-1) in growth and reproduction in female brown house snakes (*Lamprophis fuliginosus*). Gen. Comp. Endocrinol. 168, 408–414.
Sparkman, A.M., Schwartz, T.S., Madden, J.A., Boyken, S.E., Ford, N.B., Serb, J.M., Bronikowski, A.M., 2012. Rates of molecular evolution vary in vertebrates for insulin-like growth factor-1 (IGF-1), a pleiotropic locus that regulates life history traits. Gen. Comp. Endocrinol. 178, 164–173.
Sparkman, A.M., Bronikowski, A.M., Billings, J.G., Von Borstel, D., Arnold, S.J., 2013. Avian predation and the evolution of life histories in the garter snake *Thamnophis elegans*. Am. Midl. Nat. 170, 66–85.
Staroscik, A., 2004. Calculator for determining the number of copies of a template, <http://cels.uri.edu/gsc/cndna.html>. Accessed 11 August 2015.

Stearns, S.C., 1983. The influence of size and phylogeny on patterns of covariation among life-history traits in the mammals. Oikos 41, 173–187.
Stearns, S.C., 1989. Trade-offs in life-history evolution. Funct. Ecol. 3, 259–268.
Stewart, C.E., Rotwein, P., 1996. Growth, differentiation, and survival: multiple physiological functions for insulin-like growth factors. Physiol. Rev. 76, 1005–1026.
Stratikopoulos, E., Szabolcs, M., Dragatsis, I., Klinakis, A., Efstratiadis, A., 2008. The hormonal action of IGF1 in postnatal mouse growth. Proc. Natl. Acad. Sci. U.S.A. 105, 19378–19383.
Sutter, N.B., Bustamante, C.D., Chase, K., et al., 2007. A single *IGF1* allele is a major determinant of small size in dogs. Science 316, 112–115.
Swanson, E.M., Dantzer, B., 2014. Insulin-like growth factor-1 is associated with life-history variation across Mammalia. Proc. R. Soc. B 281, 20132458.
Tatar, M., Bartke, A., Antebi, A., 2003. The endocrine regulation of aging by insulin-like signals. Science 299, 1346–1350.
Vong, Q.P., Chan, K.M., Cheng, C.H.K., 2003. Quantification of common carp (*Cyprinus carpio*) IGF-I and IGF-II mRNA by real-time PCR: differential regulation of expression by GH. J. Endocrinol. 178, 513–521.
Wolf, E., Hoeflich, A., Lahm, H., 1998. What is the function of IGF-II in postnatal life? Answers from transgenic mouse models. Growth Horm. IGF Res. 8, 185–193.
Wood, A.W., Duan, C., Bern, H.A., 2005. Insulin-like growth factor signaling in fish. Int. Rev. Cytol. 243, 215–285.
Yadavalli, S., Kumar, A., Nadimpalli, S., 2009. Reptilian MPR 300 is also the IGF-IIR: cloning, sequencing and functional characterization of the IGF-II binding domain. Int. J. Biol. Macromol. 44, 435–440.
Yakar, S., Liu, J.L., Stannard, B., Butler, A., Accili, D., Sauer, B., LeRoith, D., 1999. Normal growth and development in the absence of hepatic insulin-like growth factor I. Proc. Natl. Acad. Sci. U.S.A. 96, 7324–7329.